

PHYSICAL METALLURGY  
AND HEAT TREATMENT

# Bulk Metallic Glasses: Fabrication, Structure, and Structural Changes under Heating

D. V. Louzguine<sup>a,\*</sup> and V. I. Pol'kin<sup>b,\*\*</sup>

<sup>a</sup>WPI Advanced Institute for Materials Research, Tohoku University, Sendai, 980-8577, Japan

<sup>b</sup>National University of Science and Technology "MISIS", Leninskii pr. 4, Moscow, 119049 Russia

\*e-mail: dml@wpi-aimr.tohoku.ac.jp

\*\*e-mail: vipolkin@gmail.com

Received March 27, 2015; accepted for publication April 16, 2015

**Abstract**—Bulk metallic glasses (BMGs) of Pd–Cu–Si and Pd–Ni–P systems were formed from a melt in the 1970s–1980s. However, in view of the extremely high cost of the main component (palladium), they have been outside the realm of special interest of scientists and engineers for a long time. Relatively recently, BMGs in the form of macroscopic-sized ingots have been fabricated in alloys based on industrial metals (iron, copper, magnesium, and titanium), which opened up wide possibilities for their application. BMGs possess high strength, hardness, wear resistance, elastic deformation, and corrosion resistance. In this study, a review of publications is presented and main scientific achievements in this field are described. It is noted that main scientific problems, which are not solved completely, are describing the BMG structure as well as vitrification and plastic deformation, while the technical problem attracting the attention of scientists in many countries is to increase the plasticity and impact fracture toughness of these materials.

**Keywords:** bulk metallic glasses, structure, vitrification, strength, ductility

**DOI:** 10.3103/S1067821216010107

## INTRODUCTION

Natural oxide glasses are easily formed during melt cooling, while industrial metallic alloys have a crystal-line structure in the cast stage. Excluding earlier studies on the thin-film deposition on cooled substrates in vacuum from the gas phase [1], the first samples of amorphous/glassy metallic alloys, or metallic glasses, were acquired at the turn of the 1960s by rapid melt cooling starting from the Au–Si sample of the eutectic composition [2]. This became possible due to the development of methods of very fast (with rates on the order of  $10^6$  K/s) cooling of the liquid melts, to which we can refer spinning for example. This process includes rapid (compared with usual metallurgical methods) melt solidification on a rotating copper disc/drum or upon the compression of the melt drop between two metallic plates.

In the course of casting, metallic alloys continuously transfer into the amorphous/vitreous<sup>1</sup> state upon cooling and undergo the reverse transformation under subsequent heating with a rather high rate. Metallic glasses are thermodynamically unstable relative to

crystallization [3]. They are formed because of the retardation of kinetic processes at low temperatures. Starting from the 1970s, Pd–Cu–Si and Pd–Ni–P alloys were for a long time known as samples of metallic glasses with glass-forming ability (GFA) and a critical size (as a rule, diameter of the cylindrical casting) that was largest for that time (the maximal diameter at which a uniform amorphous structure is formed) and constituting 1–2 mm [4].

Samples that are more massive were fabricated in the 1980s after melt treatment by  $B_2O_3$  flux, which made it possible to suppress the heterogeneous nucleation of crystals [5]; however, in view of the exclusively high cost of the main component (palladium), they were not especially interesting for scientists and engineers for a long time. Subsequently, the high liability of certain alloys to vitrification when using various solidification procedures made it possible to fabricate bulk metallic glasses (BMGs) with a minimal size on the order of  $10^0$ – $10^2$  mm in all three spatial dimensions [6, 7] (Fig. 1). Sizes  $\geq 1$  mm in all three spatial dimensions characterize a macroscopic sample.

Another important characteristic associated with the sample diameter is the critical cooling rate<sup>2</sup> at

<sup>1</sup> Amorphous and vitreous states are somewhat synonyms. Alloys prepared by rapid melt cooling are usually called vitreous, while amorphous materials can be prepared by other methods such as mechanical milling, ion bombardment, magnetron sputtering, electrochemical deposition, etc. It should be noted that other materials, for example, spin glasses, are not considered in this study.

<sup>2</sup> We should understand that the ingot is cooled with a continuous decrease in the cooling rate. Uniform melt cooling with a definite rate is attained by special methods, for example, with the use of controllable cooling in the differential calorimeter cell.



**Fig. 1.** Installation for gravitational casting of the melt heated with the help of an inductor into copper molds in vacuum or argon. Photograph is presented by authority of the Department of Materials Science of Nonferrous Metals at the National University of Science and Technology MISiS. Molds and BMG castings are seen on a table.

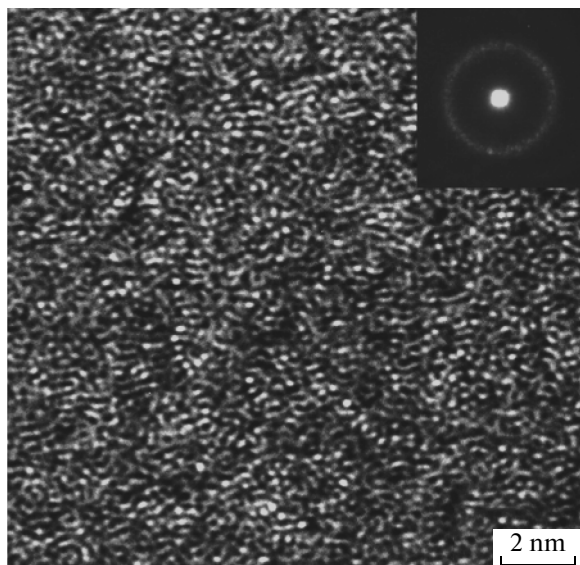


**Fig. 2.** Typical high-resolution TEM image demonstrating the absence of crystallographic planes and nanoparticles in the zirconium-based BMG. Nanobeam diffraction pattern with a probe size of  $\sim 1$  nm is shown in inset.

which crystallization is not still started. It is associated with the location of the minimum of the isothermal phase transformation diagram, TTT (time–temperature–transformation, *C*-curve) in time, or, more exactly, of the “nose” of the phase transformation diagram under continuous cooling.

### BMG FABRICATION

Depending on the vitrifying ability, metallic glasses can be fabricated using various methods. Materials with a very low GFA, including certain pure metals, can be prepared in an amorphous state by condensation from the gas phase on a substrate at room or cryo-

genic temperature [1], which is ineffective to fabricate macroscopic samples. Certain alloys in the amorphous state are prepared by mechanical stirring, for example, by milling in a ball mill [8] with further sintering or by intense plastic deformation [9]. The electrolytic deposition from solutions can be also used [10]. These methods are more effective but require large power inputs, and the alloy can be contaminated by the material of the vessel in which stirring was performed in the first case or by impurities from the solution in the second case.

Melt casting into a copper mold under gravity with the furnace sole inclination (Fig. 1) or by spraying under excess pressure in inert gas, which provides cooling with a rate of  $10^2$ – $10^3$  K/s, is much more productive. Alloys with the lower GFA are produced in the form of thin ribbons by cooling on a rapidly rotating copper disc or by other similar methods of the rapid melt with a cooling rate on the order of  $10^5$ – $10^6$  K/s.

### STRUCTURE

The presence of long-range order in the atomic arrangement, unit cell, and translation symmetry is characteristic of crystals, while the unit cell in a three-dimensional space is absent or infinite-sized for quasicrystals, but the rotational symmetry is present; on the contrary, the structure of metallic glasses looks shapeless (amorphous) at first glance and resembles the structure of liquid metals [11], which is characterized by the absence of long-range order and presence of short-range order in the atomic arrangement in the first coordination sphere (CS), as well as the medium-range order, which touches the atomic arrangement in the second and several subsequent CSs. In addition, the topological (geometric atomic arrangement) and chemical (atomic arrangement associated with tendency to form chemical bonds between elements) short-range orders are distinguished.

The structure of metallic glasses was investigated by high-resolution transmission electron microscopy (TEM) (Fig. 2) and X-ray, neutron, and electron diffraction (see, for example, [12, 13]). The BMG structure was initially described based on random dense atomic packing [14], which, however, does not make it possible to attain the actual density of metallic glasses, which is very close to their density in the crystalline state. In addition, this model does not describe the alloy structure with a strongly pronounced chemical short-range order.

A high degree of middle-range order agrees well with models that predict that the BMG structure is dense packing of atomic clusters rather than the random atomic packing [15, 16]. The clusters were observed with the help of scanning tunnel microscopy [17], by electron diffraction from a nanodimensional region (see inset in Fig. 2), and from regions several angstroms in size [18]. Metallic glasses based on Cu, Zr, and Pd possess a dense structure with a high degree

of short-range and middle-range orders, which are held for a distance of approximately 2 nm [19]. It is also shown that the short-range and middle-range orders of certain crystalline structures can serve the basis for the structure of corresponding BMGs [20].

In situ X-ray diffractometry in the transmission synchrotron radiation made it possible to reveal the structural variations in the atomic structure of the  $\text{Pd}_{42.5}\text{Cu}_{30}\text{Ni}_{7.5}\text{P}_{20}$  alloy in the supercooled liquid region and in the glass-transition range [21]. According to the radial distribution function, an increase in the interatomic distance in the first CS (with is rather unexpected and evidences the active structural reconstruction in liquid) and its decrease in the second CS, as should be expected, from thermal expansion, are observed upon cooling between the liquidus ( $T_l$ ) and glass-transition ( $T_g$ ) temperatures. The metallic vitreous alloy is compressed (or extended upon heating) below  $T_g$  classically according to thermal vibrations.

In addition, the formation of clusters with a centering phosphorus atom and nickel and copper atoms as its nearest neighbors covalently bound with it is found upon supercooling below  $T_l$  and near  $T_g$ . It is shown that such an effect is responsible for the “brittleness” of this liquid (a strong deviation of the temperature dependence of its viscosity from the Arrhenius law) of the  $\text{Pd}_{42.5}\text{Cu}_{30}\text{Ni}_{7.5}\text{P}_{20}$  alloy upon cooling [21]. Since the polymorphism phenomena in liquid [11] and polyamorphism phenomena in metallic glasses [22] were found upon increasing the pressure, we can assume the certain uniqueness of the liquid and glass structure in a certain range of thermodynamic quantities.

### GLASS-TRANSITION PHENOMENON

The vitrification phenomenon is associated with the alloy transition from liquid into glass in a certain temperature range (Fig. 3), which corresponds to the inflection point in the temperature dependence of the specific volume or alloy enthalpy. The inflection point corresponds to the glass-transition temperature ( $T_g$ ), which increases as the cooling rate increases. It is also determined by the temperature of the reverse transition into the liquid state (devitrification) during heating.

It should be noted that, strictly speaking, vitrification occurs in the limits of a narrow temperature range near  $T_g$ , which is determined as one of the inflection points<sup>3</sup> where viscosity varies by two orders of magnitude, for example, from  $10^{10}$  to  $10^{12}$  Pa s similarly to the  $\text{Cu}_{36}\text{Zr}_{48}\text{Al}_8\text{Ag}_8$  alloy [23]. Moreover, the magnitude of  $T_g$  depends on the cooling or heating rate. However, step-by-step scanning in the differential calorimeter reveals the presence of one devitrification process upon heating the four-component Zr–Cu–

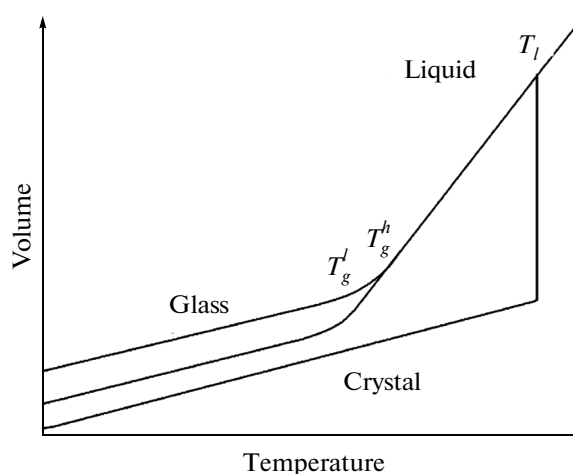


**Fig. 3.** Schematic temperature dependence of the specific (or absolute) alloy volume during crystallization somewhat below the liquidus temperature ( $T_l$ ), which conditions the jumplike variation in volume, as well as during vitrification with high and low cooling rates, which leads to corresponding inflection points in plots denoted as  $T_g^h$  and  $T_g^l$ . The higher the cooling rate is, the higher the transition temperature into the vitreous state is.

Ni–Al BMG [24] in accordance with diffusivities decreasing in the Ni–Cu–Al–Zr series.

An important question remains incompletely resolved: whether or not the metallic glass and liquid are the same phase in essence but observed at various temperatures, or if the phase transition from the liquid state into glass occurs and vice versa and, if this is the case, what kind of transition is this? At least three explanations were proposed (see, for example, [25, 26]):

(i) the vitreous phase is a supercooled (“frozen”) liquid and vitrification is simply a kinetic phenomenon rather than a thermodynamic phase transition (this viewpoint is most popular);

(ii) vitrification can be a second-order phase transition as it follows from the form of temperature dependences of thermodynamic parameters since the specific volume or enthalpy are continuous at the glass transition temperature, while their first derivatives with respect to temperature undergo discontinuity (in a certain approximation) at  $T_g$ ;

(iii) vitrification can be a first-order phase transition associated with the catastrophic behavior of entropy of liquid when its value becomes lower than the entropy of the corresponding crystal [27].

Indeed, an abrupt variation in thermodynamic parameters is not obligatory for the first-order phase transition if the local chemical composition varies gradually or the phase transition follows the shear mechanism [28].

<sup>3</sup> According to the alternative-arbitrary definition,  $T_g$  corresponds to the temperature at which melt viscosity reaches  $10^{12}$  Pa s.

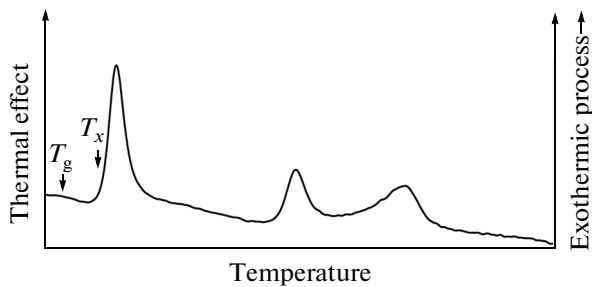


**Fig. 4.** Differential scanning calorimetry curve during heating the metallic glass. Supercooled liquid is formed at  $T_g$  and, starting from  $T_x$ , the three-step transition into the crystalline state through the formation of metastable phases occurs.

### ALLOY LIABILITY TO VITRIFICATION

The BMGs are found in binary, ternary, quaternary, and multicomponent alloys [6, 29]. Binary BMGs are formed in a very narrow composition range, and their GFA is low; however, the introduction of a definite third component considerably increases this characteristic [30].

The BMGs are formed in alloys with a high ratio  $T_g/T_l \geq 0.6$  (however, its lower value is also observed for certain alloys). Despite the fact that characteristic  $T_g/T_l$  reflects the glass-forming ability of many alloys well, a strong deviation from following this criterion is found for certain materials [30]. It should be noted that the “brittleness” of liquid [31], which is determined by the deviation of the temperature dependence of viscosity of the supercooled melt from the Arrhenius law, also plays an important role in evaluating the GFA similarly to ratio  $T_g/T_l$  [32, 33]. For example, it is responsible for low GFA of nickel despite its possibly high  $T_g$  determined by the thermal expansion of liquid and solid phases, as well as with the help of computer modeling [34]. The presence of a correlation between the Poisson coefficient and the brittleness index of the corresponding liquid is also seen [35].

Along with this, it was shown that the width of the supercooled liquid region  $\Delta T_x = T_x - T_g$  ( $T_x$  is the crystallization onset temperature), which is the index of its stability with respect to crystallization, also correlates well with the GFA [6]. The wider the occurrence region of metastable supercooled liquid is, the higher its stability with respect to crystallization is (Fig. 4).

Parameter  $\gamma = T_x/(T_g + T_l)$  [36] associates criteria  $\Delta T_x$  and  $T_g/T_l$  and provides a more reliable correlation with the experimental data. Numerous similar parameters to evaluate GFA were developed based on it [37]. Parameter  $\alpha$ , which takes into account the temperature range of alloy crystallization  $T_l - T_s$ , where  $T_s$  is the solidus temperature,  $\alpha = (T_s - T_g)/(T_l - T_g)$ , should be mentioned separately [38]. The criterion of volume difference [39]  $\delta = \alpha \rho_l (T_m - 298)/\Delta \rho_{s-l}$  [40] was also proposed. It can be illustrated by the temper-

ature dependence of specific volume ( $V = 1/\rho$ ) (Fig. 3) and associates  $\alpha_l$ , the linear expansion coefficient of cooled liquid;  $\rho$ , the liquid density;  $T_m$ , the melting point in the absolute scale; and  $\Delta \rho_{s-l}$ , the density difference between the solid crystalline and liquid phases.

The thermal conductivity of the liquid alloy also affects the cooling rate [40] (at the corresponding Bio criterion) and, consequently, GFA [41]. The electronegativity of alloying elements [42] and ratios of atomic radii [43] are also important factors affecting the GFA and the occurrence temperature range of supercooled liquid.

The assumption was also put forward that the GFA can depend on the electron concentration, which is the ratio of the number of valent electrons to the number of atoms ( $e/a$ ) [44] by analogy with the Hume–Rothery phases. However, it is not so simple to determine what value of  $e/a$  is appropriate in each concrete case, since many BMGs contain transition metals possessing the variable valence.

### STRUCTURAL VARIATIONS UPON HEATING

All macroscopic glasses prepared in the form of thin films, ribbons, or macroscopic samples possess increased free energy and are subjected to structural relaxation [45, 46], leading to their densification upon heating to temperatures below  $T_g$ , which is not the phase transformation. Structural relaxation leads to an increase in density and viscosity of metallic glass [47, 48], its embrittlement (with certain exclusions [49]), and a variation in many other properties.

However, BMGs can be considered metastable materials, since the energy barrier should be overcome for the transition into a stable crystalline state upon heating above the crystallization temperature ( $T_x$ ), which is independent of the heating rate of the sample similarly to  $T_g$ . Several metastable states of both crystalline (see, for example, peaks in Fig. 4) and quasi-crystalline phases can be fixed in this case.

The change in the phase state during crystallization is revealed by X-ray structural analysis (Fig. 5). The X-ray diffraction pattern of metallic glass contains no clear diffraction maxima, excluding peaks with a full width at half-maximum of the first of them of about  $5^\circ$ – $6^\circ$  (Fig. 5a). The less spread but rather broad maxima correspond to the formation of the nanostructured quasi-crystalline phase (Fig. 5b), while narrow peaks correspond to microscopic-sized phases, which are formed at later crystallization stages (Figs. 5c, 5d) [50].

The BMG crystallization method is widely used to fabricate nanomaterials with a small grain (particle) size from 1 to 100 nm (Fig. 6). Nanostructured alloys are most often fabricated in the course of the primary crystallization of glasses [51, 52] with the diffusion-controlled nanoparticle growth. Such a method makes it possible to attain a very homogeneous distribution of nanoparticles in a residual vitreous matrix.

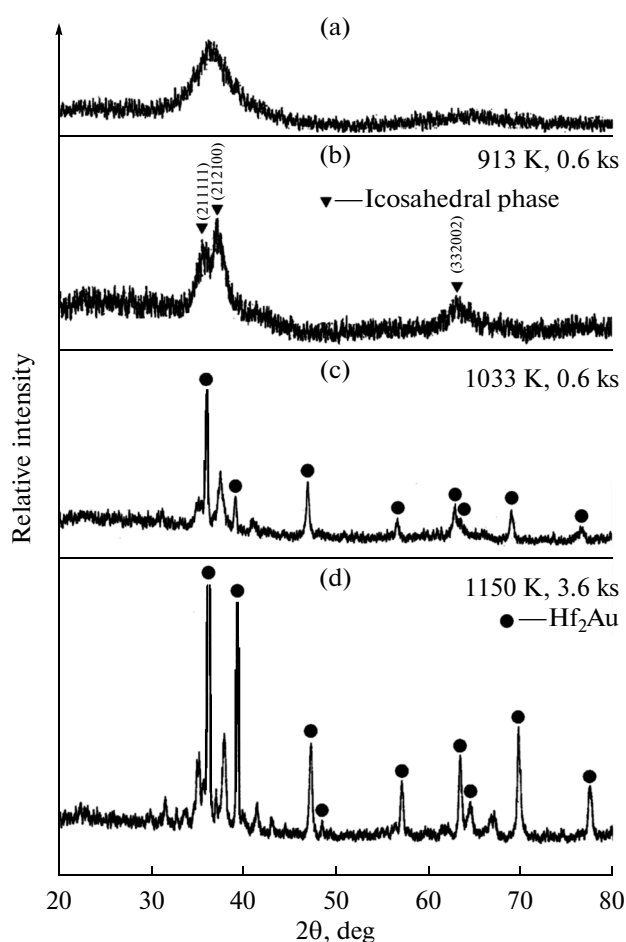


**Fig. 5.** X-ray diffraction patterns recorded from metallic glass samples of the Hf–Au–Ni–Al system (a) in the initial state and (b–d) thermally treated at various temperatures. Reprinted by authority of Elsevier [50].

Nanostructured materials are similar with “aging” crystalline alloys, in which the supersaturated solid solution is a matrix phase, while the matrix in nanostructured-amorphous (vitreous) materials is presented by the amorphous/vitreous phase, and they can possess improved mechanical properties when compared with single-phase metallic glasses, since nanoparticles prevent the propagation of shear deformation bands. Nanostructures can also be formed immediately during casting with a definite cooling rate, which should be nevertheless thoroughly controlled.

The formation of the supercooled liquid substantially affects the crystallization in BMGs [53]. This can be associated with the change in the local atomic structure in the supercooled liquid region because of its high atomic mobility when compared with the vitreous phase [54].

Three types of phase transformations were found during the BMG crystallization. They occur according to the following mechanisms:

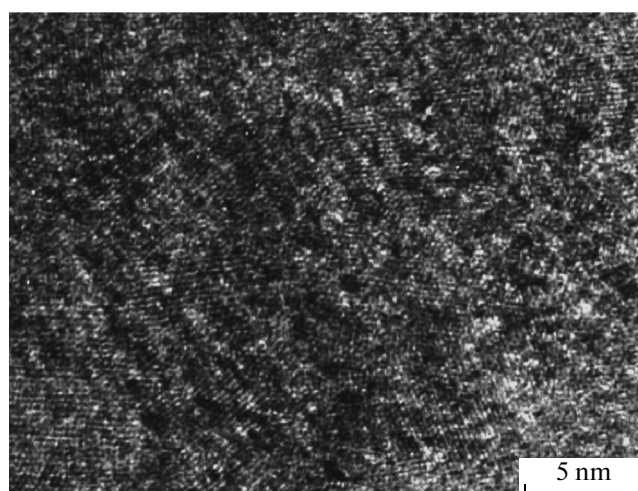


**Fig. 6.** High-resolution TEM image of the Ni–Pd–Nb–Ti–Zr alloy after the partial crystallization.

- (i) polymorphic (the isolating phase has the same composition as the initial one) [55];
- (ii) primary (the isolating phase has a composition differing from the composition of the initial vitreous phase) [56];
- (iii) eutectic (two or more phases are nucleated and they grow jointly) [57].

In addition, peritectic reactions in alloys of the glass–crystal type were found [58], while the spinodal [59] or binodal decay of supercooled liquid preceding the crystallization [60] is possible in the presence of elements with the positive heat of mixing in them.

If the crystallization follows the mechanism of nuclei formation and growth, then a considerable nucleation rate of crystallization centers, which leads to a high nuclei concentration exceeding  $10^{21} \text{ m}^{-3}$ , and a low growth rate are required to form the nanostructure [61].

When analyzing the crystallization of metallic glasses, we can use the Kolmogorov general exponential equation [62], as well as Johnson–Mehl [63] and Avrami [64] equations, for the volume fraction of the transformed substance upon the nucleation and three-dimensional nuclei growth with the limitation of the growth rate through the atomic transition through the phase interface:

$$x(t) = \frac{4\pi}{3V_0} \int_0^t I(\tau) \left[ \int_\tau^t u(t') dt' \right]^3 d\tau,$$

where  $V_0$  is the sample volume, while  $I(\tau)$  and  $u(t')$  are the time-dependent nucleation rate and nuclei growth rate, respectively. The exponent can differ from 3 if the nuclei growth is diffusion-controlled or non-three-dimensional.

The heterogeneous nucleation was observed in the  $\text{Fe}_{73.5}\text{Si}_{13.5}\text{B}_9\text{Nb}_3\text{Cu}_1$  alloy, which initially had an iso-

tropic vitreous structure. Investigations showed that Cu forms nanoclusters in its vitreous matrix, which become the sources of heterogeneous nucleation of particles of  $\alpha$ -Fe with the inclusion density of the order of  $10^{24} \text{ m}^{-3}$  with the average size of 2–3 nm [65].

Nanoparticles can be formed not only in the form of pure metals and solid solutions, but in the form of intermetallic compounds as well. For example, the crystallization of the BMG of the  $\text{Ti}_{50}\text{Ni}_{20}\text{Cu}_{23}\text{Sn}_7$  composition starts from the isolation of primary nanoparticles of the solid solution of the  $\text{Ti}_2\text{Ni}$  phase with structure cF96 [66, 67]. The extremely small size and low growth rate of  $\text{Hf}_2\text{Co}$  cF96 crystals were observed in the  $\text{Hf}_{55}\text{Co}_{25}\text{Al}_{20}$  alloy [68]. On the contrary, crystallization of the  $\text{Zr}_{55}\text{Cu}_{30}\text{Al}_{10}\text{Ni}_5$  alloy turned out very sensitive to the presence of impurities [69].

In many cases, crystallization is preceded by the redistribution of alloying elements at close distances, for example, from the formation of magnesium-enriched zones, in magnesium-based BMGs [70].

The icosahedral quasi-crystalline phase with a quasi-periodic long-range order but without the three-dimensional translational symmetry, was primarily revealed in Al–Mn alloys [71] and then in many other ones, particularly during the BMG crystallization (see Fig. 5b) [72]. In connection with this, it is revealed that, when the Ti–Zr–Ni alloy is crystallized, the smallest supercooling is required for the formation of quasi-crystals, somewhat larger supercooling is required for crystalline approximants (crystalline phases with the structure close to quasi-crystals), and the maximal one is required for usual crystalline phases [73]. A low energy barrier for the nucleation of the icosahedral phase can also explain the fact that the  $\text{Zr}_{65}\text{Al}_{7.5}\text{Ni}_{10}\text{Pd}_{17.5}$  BMG sample showed the growth of already occurring icosahedral particles upon heating [74].

Not only thermal activation but also the plastic deformation [75, 76] can cause the nanocrystallization of metallic glass. Moreover, it was also observed during the elastic deformation of the  $\text{Zr}_{62.5}\text{Cu}_{22.5}\text{Fe}_5\text{Al}_{10}$  BMG glass [77] at room temperature in conditions of the dynamic mechanical load. Crystalline diffraction maxima corresponding to the  $\text{Zr}_2\text{Fe}$  phase appeared after testing at stress  $\sigma = 586 \pm 242 \text{ MPa}$ . However, the use of a higher load ( $\sigma = 1000 \pm 200 \text{ MPa}$ ) at a frequency of 0.1 Hz in limits of the region of elastic deformation after 1000 cycles led to the nucleation of a metastable crystalline phase with elevated free energy and to an increase in crystallization enthalpy from 44 to 48 J/g [78].

Thus, nanocrystallization can be considered a consequence of inelastic effects associated with the activation of localized viscoelastic deformation regions such as shear zones, which occur even in deformation modes that are characterized by a linear character of the strain–stress curve.

## CONCLUSIONS

In this article we reviewed the publications on bulk metallic glasses with a description of the methods of their fabrication, structure of these materials, and phase transformations upon heating. These materials attract the attention of researchers in many countries, including Russia, in view of their unusual properties and structure as well as the insufficiently complete understanding of vitrification. Properties of BMGs will be considered in the subsequent review because of the limited volume of this publication.

## ACKNOWLEDGMENTS

This study was supported by the Ministry of Education and Science of the Russian Federation according to the Program of Increasing the Competitiveness of the National University of Science and Technology MISiS among Leading World Scientific-and-Educational Centers no. K2-2014-013.

## REFERENCES

1. Buckel, W. and Hilsch, R., Einfluß der Kondensation bei tiefen Temperaturen auf den elektrischen Widerstand und die Supraleitung für verschiedene Metalle, *Z. Phys.*, 1954, vol. 138, pp. 109–120.
2. Klement, W., Willens, R.H., and Duwez, P., Non-crystalline structure in solidified gold–silicon alloys, *Nature*, 1967, vol. 187, p. 869.
3. Angell, C.A., Structural instability and relaxation in liquid and glassy phases near the fragile liquid limit, *J. Non-Cryst. Solids*, 1988, vol. 102, p. 205.
4. Chen, H.S., Thermodynamic consideration on the formation and stability of metallic glass, *Acta Metall.*, 1974, vol. 22, p. 1505.
5. Kui, H.W., Greer, A.L., and Turnbull, D., Formation of bulk metallic-glass by fluxing, *Appl. Phys. Lett.*, 1984, vol. 45, p. 615.
6. Inoue, A., Stabilization of metallic supercooled liquid and bulk amorphous alloys, *Acta Mater.*, 2000, vol. 48, p. 279.
7. Johnson, W.L., Bulk glass-forming metallic alloys: science and technology, *MRS Bull.*, 1999, vol. 24, p. 42.
8. Cherdyn'tsev, V.V., Kaloshkin, S.D., and Tomilin, I.A., Interaction of iron powder with air oxygen during mechanical activation, *Fiz. Met. Metalloved.*, 1998, vol. 86, no. 6, pp. 84–89.
9. Glezer, A.M., Sundeev, R.V., and A. V. Shalimova, A.V., Tendency of metallic crystals to amorphization in the process of severe (megaplastic) deformation, *Dokl. Phys.*, 2012, vol. 57, no. 11, pp. 435–438.
10. Yamasaki, T., Schlossmacher, P., Ehrlich, K., and Ogino, Y., Formation of amorphous electrodeposited Ni–W alloys and their nanocrystallization, *Nanostruct. Mater.*, 1998, vol. 10, p. 375.
11. Brazhkin, V.V., Voloshin, R.N., Lyapin, A.G., and Popova, S.V., Quasi-transitions in simple liquid under high pressures, *Usp. Fiz. Nauk*, 1999, vol. 169, pp. 1035–1039.

12. Matsubara, E. and Waseda, Y., Structural studies of new metallic amorphous alloys with wide supercooled liquid region, *Mater. Trans. JIM*, 1995, vol. 36, p. 883.
13. Louzguine-Luzgin, D.V., Antonowicz, J., Georganakis, K., Vaughan, G., Yavari, A.R., and Inoue, A., Real-space structural studies of Cu–Zr–Ti glassy alloy, *J. Alloys Compd.*, 2008, vol. 466, p. 106.
14. Bernal, J.D., Geometry of the structure of monoatomic liquids, *Nature*, 1960, vol. 185, p. 68.
15. Miracle, D.B., The efficient cluster packing model—an atomic structural model for metallic glasses, *Acta Mater.*, 2006, vol. 54, p. 4317.
16. Sheng, H.W., Luo, W.K., Alamgir, F.M., Bai, J.M., and Ma, E., Atomic packing and short-to-medium-range order in metallic glasses, *Nature*, 2006, vol. 439, p. 419.
17. Oreshkin, A.I., Mantsevich, V.N., Savinov, S.V., Oreshkin, S.I., Panov, V.I., Maslova, N.S., and Louzguine-Luzgin, D.V., Direct visualization of Ni–Nb bulk metallic glasses surface: from initial nucleation to full crystallization, *Appl. Phys. Lett.*, 2012, vol. 101, no. 18, p. 181601.
18. Hirata, A., Kang, L.J., Fujita, T., Klumov, B., Matsue, K., Kotani, M., Yavari, A.R., and Chen, M.W., Direct observation of local atomic order in a metallic glass, *Science*, 2013, vol. 341, pp. 376–379.
19. Hirata, A., Hirotsu, Y., Ohkubo, T., Tanaka, N., and Nieh, T.G., Local atomic structure of Pd–Ni–P bulk metallic glass investigated by high-resolution electron microscopy and electron diffraction, *Intermetallics*, 2006, vol. 14, nos. 8–9, p. 903.
20. Louzguine-Luzgin, D.V., Yavari, A.R., Vaughan, G., and Inoue, A., Clustered crystalline structures as glassy phase approximants, *Intermetallics*, 2009, vol. 17, no. 7, pp. 477–480.
21. Louzguine-Luzgin, D.V., Belosludov, R., Yavari, A.R., Georganakis, K., Vaughan, G., Kawazoe, Y., and Egami, T., Structural basis for supercooled liquid fragility established by synchrotron-radiation method and computer simulation, *J. Appl. Phys.*, 2011, vol. 110, p. 043519.
22. Sheng, H., Liu, H., Cheng, Y., Wen, J., Lee, P.L., Luo, W., Shastri, S.D., and Ma, E., Polyamorphism in a metallic glass, *Nat. Mater.*, 2007, vol. 6, p. 192.
23. Louzguine-Luzgin, D.V., Wada, T., Kato, H., Perepezko, J., and Inoue, A., In situ phase separation and flow behavior in the glass transition region, *Intermetallics*, 2010, vol. 18, no. 6, pp. 1235–1239.
24. Louzguine-Luzgin, D.V., Seki, I., Yamamoto, T., Kawaji, H., Suryanarayana, C., and Inoue, A., Double-stage glass transition in a metallic glass, *Phys. Rev. B*, 2010, vol. 81, p. 144202.
25. Cohen, M.H. and Grest, G.S., Liquid–glass transition: a free volume approach, *Phys. Rev.*, 1979, vol. 20, p. 1077.
26. Beukel, A., Van Den, and Sietsma, J., The glass transition as a free volume related kinetic phenomenon, *Acta Metall. Mater.*, 1990, vol. 38, p. 383.
27. Kauzmann, W., The nature of the glassy state and the behavior of liquids at low temperatures, *Chem. Rev.*, 1948, vol. 43, p. 219.
28. Louzguine-Luzgin, D.V. and Inoue, A., The outline of glass transition phenomenon derived from the viewpoint of devitrification process, *Phys. Chem. Glass.: Eur. J. Glass. Sci. Technol. Pt. B*, 2009, vol. 50, no. 1, pp. 27–30.
29. Molokanov, V.V., Petrzhik, M.I., Mikhailova, T.N., Sviridova, T.A., and Djakonova, N.P., Formation of bulk (Zr, Ti)-based metallic glasses, *J. Non-Cryst. Solids*, 1999, vols. 250–252, pp. 560–565.
30. Louzguine-Luzgin, D.V., Miracle, D.B., Louzguina-Luzgina, L., and Inoue, A., Comparative analysis of glass-formation in binary, ternary, and multicomponent alloys, *J. Appl. Phys.*, 2010, vol. 108, p. 103511.
31. Angell, C.A., Formation of glasses from liquids and biopolymers, *Science*, 1995, vol. 2, pp. 1924–1935.
32. Senkov, O., Correlation between fragility and glass-forming ability of metallic alloys, *Phys. Rev.*, 2007, vol. 76, pp. 104–202.
33. Louzguine-Luzgin, D.V., Vittrification and devitrification processes in metallic glasses, *J. Alloys Compd.*, 2014, vol. 586, pp. 2–8.
34. Louzguine-Luzgin, D.V., Belosludov, R., Saito, M., Kawazoe, Y., and Inoue, A., Glass-transition behavior of Ni: calculation, prediction, and experiment, *J. Appl. Phys.*, 2008, vol. 104, p. 123529.
35. Novikov, V.N. and Sokolov, A.P., Poisson’s ratio and fragility of glass-forming liquids, *Nature*, 2004, vol. 431, p. 961.
36. Lu, Z.P. and Liu, C.T., A new glass-forming ability criterion for bulk metallic glasses, *Acta Mater.*, 2002, vol. 50, p. 3501.
37. Suryanarayana, C., Seki, I., and Inoue, A., A critical analysis of the glass-forming ability of alloys, *J. Non-Cryst. Solids*, 2009, vol. 355, pp. 355–360.
38. Nishiyama, N. and Inoue, A., Direct comparison between critical cooling rate and some quantitative parameters for evaluation of glass-forming ability in Pd–Cu–Ni–P alloys, *Mater. Trans.*, 2002, vol. 43, p. 1913.
39. Yavari, A.R., Small volume change on melting as a new criterion for easy formation of metallic glasses, *Phys. Lett. A*, 1983, vol. 95, p. 165.
40. Louzguine-Luzgin, D.V. and Inoue, A., An extended criterion for estimation of glass-forming ability of metals, *J. Mater. Res.*, 2007, vol. 22, pp. 1378–1383.
41. Louzguine-Luzgin, D.V., Setyawan, A.D., Kato, H., and Inoue, A., Thermal conductivity of an alloy in relation to the observed cooling rate and glass-forming ability, *Philos. Mag.*, 2007, vol. 87, pp. 1845–1854.
42. Louzguine, D.V. and Inoue, A., Electronegativity of the constituent rare-earth metals as a factor stabilizing the supercooled liquid region in Al-based metallic glasses, *Appl. Phys. Lett.*, 2001, vol. 79, p. 3410.
43. Egami, T. and Waseda, Y., Atomic size effect on the formability of metallic glasses, *J. Non-Cryst. Solids*, 1984, vol. 64, p. 113.
44. Jiang, Q., Chi, B.Q., and Li, J.C., A valence electron concentration criterion for glass-formation ability of metallic liquids, *Appl. Phys. Lett.*, 2003, vol. 82, p. 2984.
45. Debenedetti, P.G. and Stillinger, F.H., Supercooled liquids and the glass transition, *Nature*, 2001, vol. 410, p. 259.
46. Louzguine, D.V., Inoue, A., Saito, M., and Waseda, Y., Structural relaxation in Ge–Cr–Al–Nd amorphous alloy, *Scr. Mater.*, 2000, vol. 42, no. 3, pp. 289–294.
47. Busch, R., The thermophysical properties of bulk metallic glass-forming liquids, *JOM*, 2000, vol. 52, p. 39.

48. Lysenko, A.V., Lyakhov, S.A., Khonik, V.A., and Yazvitskii, M.Yu., Shear viscosity of the  $\text{Pd}_{40}\text{Cu}_{40}\text{P}_{20}$  metallic glass under conditions of isochronous heating below the glass transition temperature, *Phys. Solid State*, 2009, vol. 51, no. 2, p. 221.
49. Aljerf, M., Georarakisa, K., and Yavari, A.R., Shaping of metallic glasses by stress-annealing without thermal embrittlement, *Acta Mater.*, 2011, vol. 59, p. 3817.
50. Louzguine, D.V., Ko, M.S., and Inoue, A., Nanoscale icosahedral phase produced by devitrification of Hf–Au–Ni–Al and Hf–Au–Cu–Al metallic glasses, *Scr. Mater.*, 2001, vol. 44, pp. 637–642.
51. Abrosimova, G.E., Aronin, A.S., and Zver'kova, I.I., Phase transformations during crystallization of amorphous alloys, *Fiz. Met. Metalloved.*, 2002, vol. 94, pp. 1–6.
52. Greer, A.L., Metallic glasses, *Science*, 1995, vol. 267, p. 1947.
53. Louzguine, D.V. and Inoue, A., Influence of a supercooled liquid on devitrification of Cu-, Hf- and Ni-based metallic glasses, *Mater. Sci. Eng. A*, 2004, vols. 375–377, p. 346.
54. Louzguine, D.V. and Inoue, A., Crystallization behaviour of Al-based metallic glasses below and above the glass-transition temperature, *J. Non-Cryst. Solids*, 2002, vol. 311, no. 3, pp. 283–293.
55. Louzguine, D.V. and Inoue, A., Crystallization behavior of  $\text{Ti}_{50}\text{Ni}_{25}\text{Cu}_{25}$  amorphous alloy, *J. Mater. Sci.*, 2000, vol. 35, no. 16, pp. 4159–4164.
56. Louzguine, D.V. and Inoue, A., Nanoparticles with icosahedral symmetry in Cu-based bulk glass former induced by Pd addition, *Scr. Mater.*, 2003, vol. 48, p. 1325.
57. Louzguine-Luzgin, D.V., Xie, G., Zhang, Q., and Inoue, A., Effect of Fe on the glass-forming ability, structure and devitrification behavior of Zr–Cu–Al bulk glass-forming alloys, *Phil. Mag.*, 2010, vol. 90, no. 14, pp. 1955–1968.
58. Louzguine-Luzgin, D.V., Kaloshkin, S.D., and Inoue, A., Peritectic-like reactions involving glassy phase, *Rev. Advan. Mater. Sci.*, 2008, vol. 18, pp. 653–659.
59. Kim, D.H., Kim, W.T., Park, E.S., Mattern, N., and Eckert, J., Phase separation in metallic glasses, *Progr. Mater. Sci.*, 2013, vol. 58, pp. 1103–1172.
60. Louzguine-Luzgin, D.V., Wada, T., Kato, H., Perepezko, J., and Inoue, A., In situ phase separation and flow behavior in the glass transition region, *Intermetallics*, 2010, vol. 18, no. 6, pp. 1235–1239.
61. Perepezko, J.H. and Hebert, R.J., Amorphous aluminum alloys—synthesis and stability, *J. Metall.*, 2002, vol. 54, p. 34.
62. Kolmogorov, A.N., On statistic theory of crystallization, *Izv. Akad. Nauk SSSR, Ser. Mat.*, 1937, vol. 3, p. 355.
63. Johnson, M.W.A. and Mehl, K.F., Reaction kinetics in processes of nucleation and growth, *Trans. Amer. Inst. Mining. Met. Eng.*, 1939, vol. 135, p. 416.
64. Avrami, M., Kinetics of phase change III: granulation, phase change an microstructures, *J. Chem. Phys.*, 1941, vol. 9, p. 177.
65. Hono, K., Hiraga, K., Wang, Q., Inoue, A., and Sakurai, T., The microstructure evolution of a  $\text{Fe}_{73.5}\text{Si}_{13.5}\text{B}_9\text{Nb}_3\text{Cu}_1$  nanocrystalline soft magnetic material, *Acta Metall. Mater.*, 1992, vol. 40, p. 2137.
66. Louzguine, D.V. and Inoue, A., Nanocrystallization of Ti–Ni–Cu–Sn amorphous alloy, *Scr. Mater.*, 2000, vol. 43, p. 371.
67. He, G., Eckert, J., and Loser, W., Stability, phase transformation and deformation behavior of Ti-base metallic glass and composites, *Acta Mater.*, 2003, vol. 51, p. 1621.
68. Louzguine, D.V., Kato, H., Kim, H.S., and Inoue, A., Formation of 2–5 nm size pre-precipitates of cF96 phase in a Hf–Co–Al glassy alloy, *J. Alloys Compd.*, 2003, vol. 359, pp. 198–201.
69. Louzguine-Luzgin, D.V., Suryanarayana, C., Saito, T., Zhang, Q., Chen, N., Saida, J., and Inoue, A., Unusual solidification behavior of a Zr–Cu–Ni–Al bulk glassy alloy made from low-purity Zr, *Intermetallics*, 2010, vol. 18, no. 8, p. 1531.
70. Louzguine, D.V., Louzguina, L.V., and Inoue, A., Multistage devitrification of Mg–Ni–Mm and Mg–Ni–Mm metallic glasses (Mm = mischmetal), *Phil. Mag.*, 2003, vol. 83, p. 203.
71. Shechtman, D., Blech, L.A., Gratias, D., and Cahn, J.W., Metallic phase with long-range orientational order and no translational symmetry, *Phys. Rev. Lett.*, 1984, vol. 53, p. 1951.
72. Louzguine-Luzgin, D.V. and Inoue, A., Formation and properties of quasicrystals, *Ann. Rev. Mater. Res.*, 2008, vol. 38, pp. 403–423.
73. Kelton, K.F., Gangopadhyay, A.K., Lee, G.W., Hanne, L., Hyers, R.W., Krishnan, S., Robinson, M.B., Rogers, J., and Rathz, T.J., X-ray and electrostatic levitation undercooling studies in Ti–Zr–Ni quasicrystal forming alloys, *J. Non-Cryst. Solids*, 2002, vol. 312–314, p. 305.
74. Louzguine-Luzgin, D.V., Zeng, Y., Setyawan, A.D.H., Nishiyama, N., Kato, H., Saida, J., and Inoue, A., Deformation behavior of Zr- and Ni-based bulk glassy alloys, *J. Mater. Res.*, 2007, vol. 22, p. 1087.
75. Glezer, A.M., Sundeev, R.V., Shalimova, A.V., and Useinov, S.S., Tendency of metallic crystals to amorphization in the process of severe (megaplastic) deformation, *Russ. Phys. J.*, 2012, vol. 54, pp. 898–905.
76. Oak, J.J., Louzguine-Luzgin, D.V., and Inoue, A., Investigation of glass-forming ability, deformation and corrosion behavior of Ni-free Ti-based BMG alloys designed for application as dental implants, *Mater. Sci. Eng.*, 2009, vol. 29, p. 2009.
77. Caron, A., Kawashima, A., Fecht, H.J., and Louzguine-Luzgin, D.V., On the anelasticity and strain induced structural changes in a Zr-based bulk metallic glass, *Appl. Phys. Lett.*, 2011, vol. 99, p. 171907.
78. Churyumov, A.Yu., Bazlov, A.I., Zadorozhnyy, V.Yu., Solonin, A.N., Caron, A., and Louzguine-Luzgin, D.V., Phase transformations in Zr-based bulk metallic glass cyclically loaded before plastic yielding, *Mater. Sci. Eng. A*, 2012, vol. 550, pp. 358–362.

Translated by N. Korovin